

## The discovery of high- $T_c$ superconductivity-unexpected discovery, unconventional behaviour

A Andreone<sup>1</sup>, A Barone<sup>2</sup>, F Lombardi<sup>3</sup> and F Tafuri<sup>4</sup>

1. CNISM and Dipartimento di Scienze Fisiche, Università di Napoli "Federico II", Napoli, Italy

2. CNR-INFM "coherentia" and Dipartimento di Scienze Fisiche, Università di Napoli "Federico II", Napoli, Italy

3. Quantum Device Physics Laboratory, Department of Microtechnology and Nanoscience, MC2, Chalmers University of Technology, S-412 96 Göteborg, Sweden

4. CNR-INFM "coherentia" and Dipartimento Ingegneria dell'Informazione, Seconda Università di Napoli Aversa (CE), Italy

(Received 25 June 2006; accepted 29 July 2006)

### Abstract

A brief review on some peculiar properties of high temperature superconductors (HTS) is presented. Twenty years after the discovery, it appears more and more clear that the behaviour of this new class of materials is remarkably different from what have been re-classified as "conventional" superconductors. In the following we will focus our attention on the study of two phenomena, namely the Josephson effect and the Meissner effect, where the unconventional nature of superconductivity in HTS offers exciting perspectives both for the understanding of the underlying mechanism, so far still unknown, and for the large potential of applications in different areas of superconducting electronics.

**Keywords:** high temperature superconductors, Josephson effect, macroscopic quantum tunneling, electrodynamic response, Meissner effect

### 1. Introduction

It is obviously mistaken to consider high- $T_c$  superconductors just as superconductors with a higher  $T_c$ . The pretence of giving even just a bird's eye view of the whole panorama of structural and functional aspects of the class of high critical temperature superconducting materials and the variety of related implications and applications would be too ambitious. Our task is limited to the presentation of a few examples among the variety of intriguing aspects and important achievements which has characterized the discovery of Bednorz and Müller [1] from that time on. As for the materials, it was obviously of paramount interest was also the discovery of the superconducting state in the  $Y_1Ba_2Cu_3O_{7-\delta}$  compound [2], the first one whose critical temperature exceeded the liquid nitrogen temperature. In the following the interest of the scientific community was captured also by the increase of the high  $T_c$  superconductors family and to the relativity "less unconventional" material such as  $MgB_2$ . In this work we review aspects of two main subjects: the physics of high- $T_c$  Josephson effect and the electrodynamic response of high- $T_c$  materials.

Ever since the discovery of high critical temperature superconductors (HTS), as far as the Josephson effect is concerned [3], the fabrication of high quality junctions

has presented a difficult materials science task. The goal of producing a tri-layer structure, which could reproduce the very successful achievements of low critical temperature superconductor (S) junctions, with an insulating (I) barrier (S-I-S), was always aimed at, but never really pursued in a systematic and reliable way. This situation reflected the structural complexity of HTS, and the difficulty of finding a good material science recipe for growing a barrier on a highly non-uniform HTS electrode, which was also characterized by poor surface superconducting properties. Aspects of this topic will be briefly discussed in section 2.

As for the electrodynamic response of HTS, its measurement has been since the discovery of cuprates an important probe of the microscopic mechanisms responsible of the superconducting state. Studying how the material under test behaves in the presence of an e.m. field incident on its surface has been used during the years to yield information on the nature of quasiparticles in the superconducting state, their scattering, density of states, and, if a more sophisticated analysis is undertaken, on the superconducting pairing mechanism in these materials. In section 3 we will briefly summarise two phenomena where a clear distinction appears in the behaviour of HTS and conventional superconductors, namely the linear and the nonlinear Meissner effect.

## 2. HTS Josephson structures

Despite the slow progress in material science issues related to the realization of HTS junctions, the new physical aspects which have been raised are particularly exciting. What made the novel physics interesting is mostly related to the unconventional order parameter symmetry (OPS) [4-6]. The OPS was made experimentally accessible by reproducible and good quality junctions, such as grain boundary (GB) Josephson junctions [7-8] (mostly the bicrystal and the biepitaxial technologies). In particular, double angle CeO<sub>2</sub>-based biepitaxial junctions have shown in particular ideal tunnel-like properties, crucial pre-requisites for the various experiments sketched below [9-12].

### 2.1 Towards "quantum" junctions

When considering new and exciting physical aspects associated with unconventional OPS and Josephson junctions, the idea of developing  $\pi$ -circuitry and more in particular novel designs of "quiet qubits" [13-15] is among the most fascinating. The "quiet" aspect of HTS proposals (no need to apply a constant magnetic bias, as opposed to systems based on low temperature superconductor Josephson junctions) probably represents the most relevant feature motivating the interest for HTS qubit systems. Furthermore, the concepts behind the various "qubit" proposals combine several other exciting physical aspects related to d-wave OPS, such as Andreev bound states [16], time reversal symmetry breaking [17], an imaginary component of the order parameter, and so on.

"Qubit" proposals involving high-T<sub>c</sub> superconductors [13-15] most often exploit Josephson junction circuits with an energy-phase relation with two minima in the absence of an external magnetic field, meaning that there is no need to apply a constant magnetic bias, unlike in systems based on low temperature superconductors. The most favorable configurations for two minima are offered by 45° GB and S-N-D with the d-wave electrode misoriented by 45°. Naturally degenerate states and violation of the time reversal symmetry become the keywords and concepts of all qubit proposals.

Some cautious optimism in the possibility of exploiting the intrinsic bistable properties of HTS for quantum circuitry is currently encouraged by a series of results which we summarize below.

Current vs the superconducting phase ( $I_c$ - $\varphi$ ) measurements on high angle bicrystal grain boundary junctions, especially in 45° asymmetric and 45° symmetric configurations, have reported the prevalence of the  $2\varphi$  component under some conditions [18, 19]. In RF measurements the sample is inductively coupled to a high-quality parallel resonance circuit driven at its resonant frequency. The angular phase shift between the driving current and the voltage across the circuit is measured by a rf lock-in voltmeter as a function of the external magnetic flux [18]. Other evidence comes from  $I_c$  (H) measurements on 45° bicrystal SQUIDs. The  $2\varphi$  component results in a clear deviation of the magnetic pattern, which presents regular deviations from the

expected cosine dependence. In this experiment the possibility of using size effects in sub-micron junctions has been exploited to freeze out low energy quasi-particles, and to induce a prevailing  $2\varphi$  component in the  $I_c$  -  $\varphi$  dependence [19]. A SQUID with two grain boundary junctions, chosen to have a doubly degenerate state, forming a mesoscopic island may potentially represent a silent phase qubit whose operating point is stable and protected from external field fluctuations by its symmetry [20, 21]. The read-out SQUID is proposed to be in the same high- T<sub>c</sub> film as the qubit itself.

Contributions to dissipation due to different transport processes, such as channels due to nodal quasi-particles, midgap states, or their combination, have been identified and distinguished [22]. In particular cases, de-coherence times and quality factors were calculated considering the system coupled to an ohmic heat bath. It has also been argued that problems in observing quantum effects due to the presence of gapless quasi-particle excitations can be overcome by choosing the proper working phase point [23]. In particular decoherence mechanisms can be reduced by selecting appropriate tunneling directions because of the strong phase dependence of the quasi-particle conductance in a d-wave GB junction.

The encouraging results presented in this and the next section have to be always counter-balanced by caution, which is not only due to the well-known general questions concerning any possible use of any solid-state device for quantum computation, their protocols, and the nature of superconductivity of HTS, but also to several technical problems, concerning yield and reproducibility. Even the crucial conditions to observe the  $2\varphi$  component are not well understood. As a matter of fact, a favorable quantum regime may be hindered by the lack of understanding of the junction transport processes, and of the interplay between OPS effects and barrier/microstructure effects.

It may be important to reach a regime in which "intrinsic" d-wave induced effects are isolated from "extrinsic" effects [24]. Intrinsic effects are only due to the d-wave order parameter, while extrinsic effects are mostly due to the d-wave order parameter and occur only in junctions with particular morphologies and/or properties. Examples of extrinsic effects are the anomalous dependence of the critical current on the magnetic field [25,26] and the presence of specific spontaneous currents revealed through Scanning SQUID Microscopy [24,25]. Extrinsic effects may be undesirable and even mask the features of the intrinsic effects. Double angle CeO<sub>2</sub>-based biepitaxial junctions are structures particularly versatile to exploit the HTS anisotropy and the d-wave OP [9-12].

### 2.2 YBCO biepitaxial junctions and macroscopic quantum tunneling

In this section we briefly describe biepitaxial Josephson junctions and the main ideas and outcomes of the MQT experiment. The biepitaxial Josephson junctions chosen

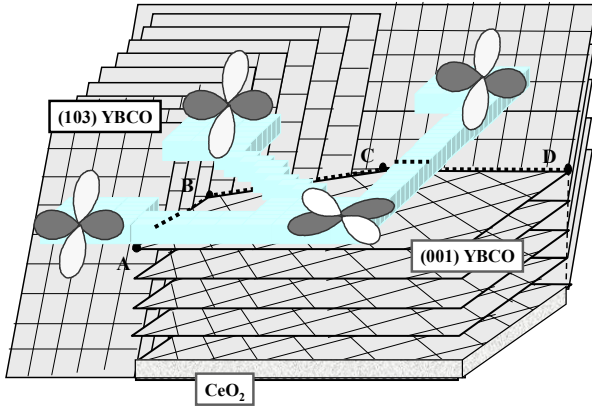


**Figure 1.** (color online) Sketch of the grain boundary structure in the bieftaxial technique.

for the MQT experiment were the result of efforts directed to produce tunnel-like junctions. In the first version, YBCO would grow along the  $c$ -axis (100) on the seed of MgO (110) oriented and along the (103) direction on the bare (110) SrTiO<sub>3</sub> substrate. In the second version CeO<sub>2</sub> replaces MgO as a seed layer. The presence of the CeO<sub>2</sub> produces an additional 45° in-plane rotation of YBCO axes with respect to the in-plane directions of the substrate. Figure 1 shows the OPS configuration for this type of configuration.

The tilt of one of the electrodes and the in-plane 45° rotation on the CeO<sub>2</sub> are the main ingredients to achieve tunnel-like barriers. They both contribute to decrease the barrier transmission and the in plane rotation enhances the desired d-wave features. A remarkable achievement has been to realize junctions whose critical current  $I_c$  depends on the interface orientation  $\theta$  in complete agreement with the predictions of a d-wave OPS [10] (see figure 2). This means that d-wave effects are dominant for some types of junctions, and robust in the sense that interface microstructure cannot mask them. Finally, this implies that we can select the junction for the MQT experiment knowing the OPS configuration exactly. Since we are as interested in those features that are distinct from the case of low  $T_c$  superconductor (LTS) junctions, namely effects due to OPS, second harmonic component, and dissipation due to low energy quasi-particles [8, 11, 12], we select the junction in the tilt configuration (angle  $\theta = 0^\circ$ ). This configuration (lobe to node) maximizes d-wave induced effects. The measurement strategy was the same used for LTS JJs [27].

We define the strength of the second harmonic components in the current-phase relation (CPR) by the parameter  $a = I_2/I_1$ , where  $I_2$  and  $I_1$  are the second and first harmonic components in the CPR respectively. This results in  $I = I_1(\sin \varphi - a \sin 2\varphi)$ . For zero bias and  $a > 0.5$  the potential has the shape of a double well. For  $a < 0.5$  the potential is single well. The analysis is restricted to  $a < 2$ ; in the case  $0.5 < a < 2$  the phase will always escape

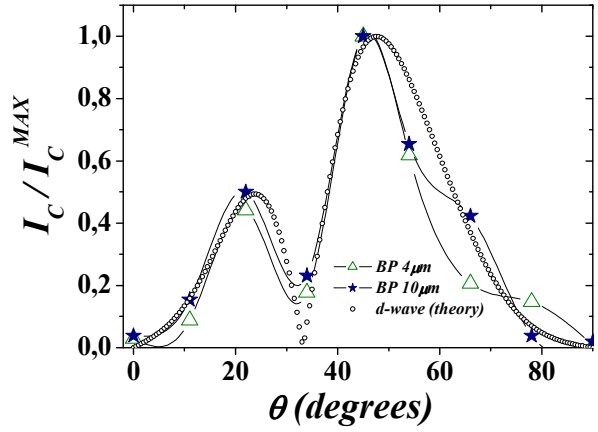


**Figure 2.** (color online) Critical current density  $J_c$  vs angle  $\theta$  for two sets of junctions prepared on the same chip, 10  $\mu m$  (triangles) and 4  $\mu m$  (stars) wide respectively ( $T = 4.2$  K). Solid lines connecting triangles and stars are guides for the eye.  $J_c$  values are normalized to their maximum ( $J_c \cong 7 \times 10^3$  A/cm<sup>2</sup> for the 10  $\mu m$  wide junctions). Experimental data are compared with predictions based on d-wave OP symmetry (dotted line).

into the running state from the lower lying well of the tilted "double-welled" washboard potential. When the bias current  $\gamma = I/I_{CO}$  is ramped from 0 to  $\gamma < 1$ , the junction is in the zero voltage state in absence of thermal and quantum fluctuations. At finite temperature, the junction may switch into a finite voltage state for a bias current  $\gamma < 1$ . This corresponds to the particle escaping from the well either by a thermally activated process or by tunneling through the barrier potential (MQT). In the pure thermal regime, the escape rate for weak to moderate damping is determined by [28]

$$\Gamma_t(a) = a_t \frac{\omega_p(a)}{2\pi} \exp\left[-\frac{\Delta U(a)}{k_B T}\right], \quad (1)$$

where,  $\omega_p(a) = c(a)^{-1/2} (2\pi I_{CO} / \Phi_0 C)^{1/2} (1 - \gamma^2)^{1/4}$  is the plasma frequency,  $a_t$  is the thermal prefactor and  $\Delta U(a) = c(a)(E_J 4\sqrt{2}/3)(1 - \gamma)^{3/2}$  is the barrier height for  $\gamma$  close to one

(with  $c(a) = \left[ \left( 0.5 + 3/2\sqrt{1 + 32a^2} \right) / 2 \right]^{1/2}$  and  $E_J = I_{CO} \Phi_0 / 2\pi$ ).

The escape rate will be dominated by MQT at low enough temperature [29]: for  $Q > 1$  and  $\gamma$  close to one it is approximated by the expression for a cubic potential [29]

$$\Gamma_q(a) = a_q \frac{\omega_p(a)}{2\pi} \exp\left[-7.2 \frac{\Delta U(a)}{\hbar \omega_p(a)} \left(1 + \frac{0.87}{Q}\right)\right], \quad (2)$$

where  $a_q = (864\pi \Delta U / \hbar \omega_p)^{1/2}$  and  $Q = \omega_p R C$  is the quality factor ( $R$  is the resistance of the junction).

For a fixed critical current  $I_{CO}$  the second harmonic (compared to the case of a pure  $\sin \varphi$ ) reduces the barrier height  $\Delta U$  and increases the plasma frequency  $\omega_p$  at bias currents  $\gamma$  close to one.

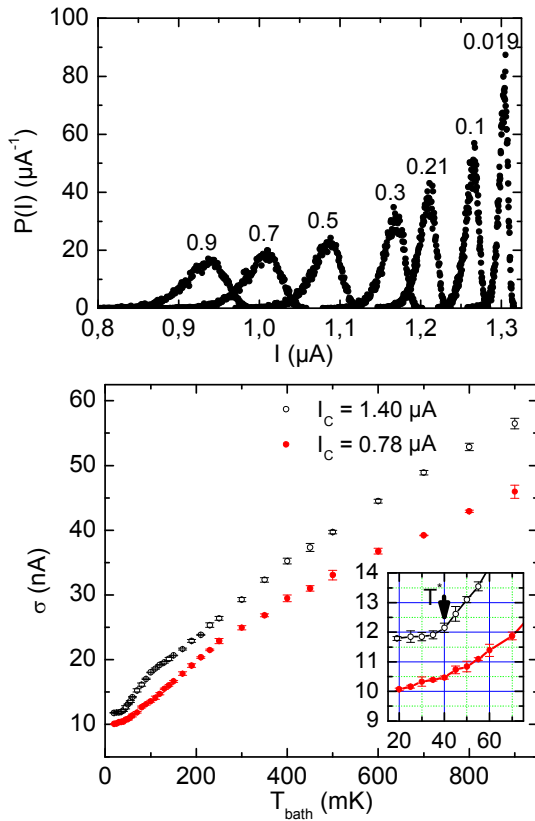


**Figure 3.** (color online) (a) Switching current probability distribution for different bath temperatures  $T_{\text{bath}}$ . The symbols represent data, and the lines are fits. (b) Temperature dependence of width  $\sigma$  for  $I_{c0}=1.40 \mu\text{A}$  and  $B=0 \text{ T}$  (open points) and  $I_{c0}=0.78 \mu\text{A}$  and  $B=2 \text{ mT}$  (full points). In the inset the low temperature part. (below 75 mK) is in evidence. Adapted from [11].

The switching current probability distributions have been measured as a function of temperature. The dependence of the distribution width  $\sigma$  on temperature is reported in figure 3. The measured  $\sigma$  saturates below 50 mK, indicating a crossover from the thermal to the MQT regime. To rule out the possibility that the saturation of  $\sigma$  is due to any spurious noise or heating in the measurement setup the switching current probability distributions was measured for a reduced critical current  $I_{c0}=0.78 \mu\text{A}$  by applying an external magnetic field  $B=2 \text{ mT}$ . The data in the presence of a magnetic field clearly show a smaller width  $\sigma$ , which does not saturate down to the base temperature [8].

The plasma frequency  $\omega_p/2\pi$  was about  $7.8 \pm 0.5 \text{ GHz}$ . The ratio between the second and first harmonics ranges from  $a \approx 0$  at  $T = 900 \text{ mK}$  to a saturated value  $a = 0.77 \pm 0.06$  below  $T = 100 \text{ mK}$ . Therefore at low temperatures the fundamental state is naturally double degenerate [11].

The low average barrier transparency ( $D \approx 10^{-4}$ ) strongly reduces dissipation from nodal quasi-particles. This is one of the main arguments to understand why dissipation mechanisms related to a d-wave order parameter in the junction do not prevent the observation

of MQT [11, 12]. The low dissipation argues against the common belief that the presence of low energy quasi-particles in HTS systems can prevent the macroscopic quantum behavior required for solid-state quantum computers. Observation of energy level quantization in the same type of d-wave Josephson junction and high quality factors has been also reported [12].

### 3. Electrodynamic response of HTS

The pairing mechanism responsible for superconductivity in HTS is still unknown. Studies of the electrodynamic properties are extremely useful in order to provide at least a phenomenological picture, revealing information regarding the pairing state, the energy gap, the density of states, and to give important insights into the mechanism of high- $T_c$  superconductivity and its difference with the standard BCS theory. In the following we will briefly review some experiments aimed to address this fundamental question, and where the response of HTS is remarkably different from conventional superconductors.

#### 3.1 Linear Meissner effect

Hardy *et al.* [30] at the University of British Columbia first demonstrated that high resolution measurements of the London penetration depth  $\lambda$  could detect the presence of nodes in the superconducting wavefunction characteristic of a d-wave symmetry. Following their pioneering work, the observation of the linear Meissner effect – via the study of the magnetic penetration depth well below  $H_{c1}$  – has become one of the main probes of the nature of the pairing state in cuprates and in other novel superconductors. Since then,  $\lambda$  measurements have been used to examine not only nodal quasiparticles but two-gap superconductivity [31], anisotropy of the energy gap [32], Andreev surface states [33], and nonlinear Meissner effect too [34], to name a few problems of current interest in the field of superconductivity.

Till today the properties of the superconducting pair condensate in the HTS have been intensively investigated in stoichiometric and optimally doped, as well as underdoped and overdoped, samples, for both hole and electron doped compounds [35]. Many reports have also shown the importance of studying the effect of disorder and doping on the superconducting properties of the cuprates. Amongst them, studies of the effect of magnetic impurities or substitutional doping on the penetration depth of films, crystals and oriented powders of superconducting oxides have been published [36-38].

Different techniques have been used to determine the superfluid density  $n_s$  (or, more correctly, the phase stiffness, proportional to  $1/\lambda^2$ ), most of them related to measurements of the penetration depth in both  $a-b$  and  $c$  direction using an inductance, microwave, or muon spin resonance techniques [29, 39, 40].

The most relevant aspect which has been investigated concerns the temperature dependence of the penetration

depth of HTS films and crystals. Data on clean hole-doped [10, 41] single crystals showed that the in-plane penetration depth  $\lambda_{ab}$  at low temperature grows linearly, which is consistent with a  $d$ -wave order parameter. For relatively small concentration of defects,  $\lambda_{ab}$  of hole-doped samples shows a  $T^2$  law at the lowest temperatures and a crossover to a linear behaviour increasing  $T$  [42]. This behaviour was at odds with the  $s$ -wave, spin-singlet wavefunction first formulated by Bardeen, Cooper and Schrieffer in 1957 [43] to explain conventional superconductivity, that is protected from the influence of defects by Anderson's theorem [44] and where an exponential  $\lambda(T)$  dependence is expected - the signature of a finite and fully isotropic energy gap. For a clean HTS sample, the behaviour at low  $T$  can be described using the well-known formula [45]

$$\Delta\lambda / \lambda(0) \approx [\ln 2 / \Delta(0)]T, \quad (3)$$

where  $\Delta\lambda = \lambda(T) - \lambda(0)$ , and  $\Delta(0)$  is the gap maximum, if we choose for the in-plane  $\mathbf{k}$  dependence of the gap function a  $d_{x^2-y^2}$  symmetry.

Since the variation of the magnetic penetration depth is proportional to the fraction of normal electrons in the low-temperature limit, it is useful to compare this quantity measured as a function of temperature in different superconductors.

Amongst the different families of cuprate superconductors, the  $Y_1Ba_2Cu_4O_8$  (Y124) system is characterized by the presence of double CuO chains per unit cell in the  $b$ -axis direction. It was early recognized that the chains play the role of charge reservoirs for hole-doping of the superconducting  $CuO_2$  planes. Although less widely studied than its celebrate counterpart, the  $Y_1Ba_2Cu_3O_{7-\delta}$  (Y123) compound, Y124 is appealing since its oxygen stoichiometry is well defined and therefore no disorder or structural inhomogeneities arising from chemical substitutions and/or oxygen vacancies are present. Thus, Y124 is a model system for studying the intrinsic effect of the reservoir layers on the electronic properties of cuprates.

In figure 4  $\Delta\lambda$  versus the reduced temperature  $t=T/T_c$  is shown for an optimally doped Y123 single crystal, a Y124 single crystal, and an epitaxial NbN thin film. At low  $t$ , both cuprates follow a linear dependence, in accordance with the  $d$ -wave model, whereas for the  $s$ -wave BCS conventional superconductor NbN the low-energy quasiparticle excitation rate is strongly reduced, consistently with its fully gapped nature.

### 3.2 Nonlinear Meissner effect

Immediately after the BCS theory came up, Bardeen showed [47] that in the presence of a superfluid velocity field  $\mathbf{v}_s$ , quasiparticles co-moving with  $\mathbf{v}_s$  are shifted up in energy whereas those moving counter to  $\mathbf{v}_s$  are shifted down. This effect is sometimes called the quasiparticle Doppler shift. For  $T > 0$  the increased population of counter-moving quasiparticles constitutes a paramagnetic current that reduces the Meissner

screening. Since  $\mathbf{v}_s$  is proportional to the applied magnetic field  $H$ , this nonlinearity produces a  $\lambda(H)$  dependence even in the Meissner state. In  $s$ -wave superconductors, the field dependent correction is extremely small since the penetration depth itself is already exponentially suppressed.

After the discovery of HTS, Yip and Sauls [48] showed theoretically that the situation would be quite different in a  $d$ -wave superconductor. The existence of nodes in the gap function implies that the Doppler shift can change the quasiparticle population at arbitrarily low temperatures.

This correction, almost negligible in  $s$ -wave superconductors, leads to an observable – in principle-linear increase in the penetration depth as a function of  $H$ . Moreover, the slope is different if the magnetic field is applied in the direction of a node or an antinode.

Since the “nonlinear Meissner effect” (NLME) results from the field-induced change in quasi-particle populations and does not include field-induced pairing breaking effects on the gap itself, it could be used both to verify the existence of nodes and to locate them on the Fermi surface.

Despite considerable experimental efforts, the NLME has proven extremely difficult to identify. This is because a large number of constraints must be satisfied, the most important one being that  $H$  must be smaller than the lower critical field, to avoid contributions from vortex motion which can also give a linear correction to  $\lambda$ . This sets a very stringent upper limit to the observable change in the penetration depth, of the order of 1% of  $\lambda(0)$ . Besides that, impurities or nonlocal effects can easily wash out the expected linear dependence.

The difficulty in providing a convincing evidence of NLME led to a re-examination of the original Yip-Sauls argument and to other suggestions for detecting nonlinear effects. Dahm and Scalapino [49] to exploit the analytic corrections to the supercurrent leading to changes in  $\lambda$  that vary as  $H^2/T$ , that are apparently less affected by impurity scattering and can be observed over a wider temperature range.

The quasiparticle backflow contribution of the NLME here lies in a nonlinear parameter  $b(T)$ , proportional to the intermodulation power arising from the superconducting material under test, that displays a different temperature behaviour depending on the gap function symmetry. Dahm and Scalapino demonstrated that this upturn would provide a clear and unique signature of the nodes in the  $d$ -wave gap and that this feature could be measured directly via microwave intermodulation effects.

In figure 5 a comparison of measurements carried out on  $s$ -wave and  $d$ -wave superconductors is reported, plotting  $b^2$  evaluated at constant circulating power as a function of temperature for Nb, and  $Y_1Ba_2Cu_3O_{7-\delta}$  [50]. In the case of Y123 thin films, the squared nonlinear parameter  $b^2$  increases as  $1/T^2$  following the prediction for the gap function of a  $d$ -wave superconductor, and in agreement also with other experiments performed

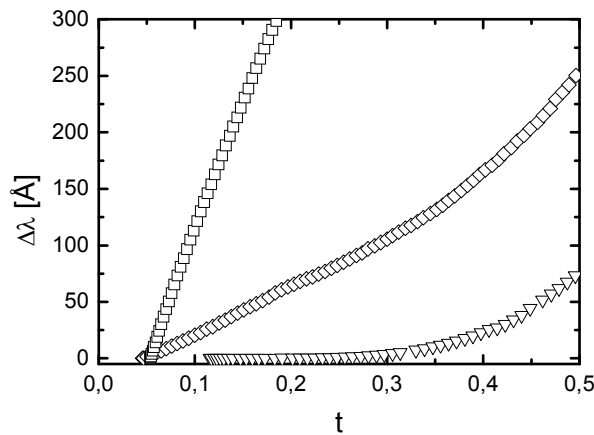


**Figure 4.** Low-temperature variation of the in-plane magnetic penetration depth for different superconductors: a Y124 single crystal ( $\square$ ), a Y123 single crystal ( $\diamond$ ), a NbN epitaxial thin film ( $\nabla$ ). Adapted from [50].

on a number of microwave stripline resonators [51].

#### 4. Conclusions

Results on the grain boundary biepitaxial Josephson junctions indicate that high quality junctions can be obtained, where advantages of the d-wave order parameter symmetry can be exploited. Achievements from experiments on macroscopic quantum tunneling and level energy quantization experiments indicate that the role of dissipation mechanisms in HTS has to be revised and d-wave devices do possess a macroscopic quantum degree of freedom, contrary to previous estimates.

Electrodynamic measurements have been proven to be a very powerful probe of the pairing state, the energy

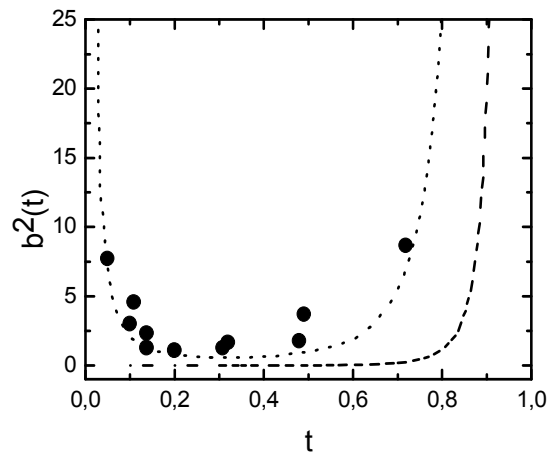


**Figure 5.** The behaviour of  $b^2$  vs the reduced temperature  $t = T/T_c$ . The dotted line represents the theoretical behaviour for the  $d$ -wave case, the solid line for the  $s$ -wave one-band case; the experimental points represent the results for standard high quality YBCO films at a circulating power of 0 dBm. Adapted from [49].

gap, and the density of states of a superconductor. The study of the behaviour of a superconductor in the presence of an e.m. field highlights the difference in the microscopic properties of HTS in respect of conventional materials. The observation of linear and nonlinear effects in the Meissner state can be successfully used to reveal the intimate unconventional nature of high- $T_c$  superconductivity.

#### Acknowledgements

This work was partially supported by PRIN '04 "Effetti quantistici in nanostrutture e dispositivi superconduttivi" and PRIN '04 "Two-gap superconductivity in MgB<sub>2</sub>: The role of disorder."

#### References

1. J G Bednorz and K A Müller, *Z. Phys. B Condensed Matter* **64** (1986) 189.
2. M K Wu, J R Ashburn, C J Torng, P H Hor, R L Meng, L Gao, Z J Huang, Y Q Wang and C W Chu, *Phys. Rev. Lett.* **58** (1987) 908.
3. A Barone and G Paternò, "Physics and Applications of the Josephson Effect", Wiley (1982).
4. M Sigrist and T M Rice, *Rev. Mod. Phys.* **67** (1995) 503.
5. D J van Harlingen, *Rev. Mod. Phys.* **67** (1995) 515.
6. C C Tsuei and J R Kirtley *Rev. Mod. Phys.* **72** (2000) 969.
7. H Hilgenkamp and J Mannhart, *Rev. Mod. Phys.* **74** (2002) 485.
8. F. Tafuri and J. R. Kirtley, *Rep. Prog. Phys.* **68** (2005) 2573.
9. F Tafuri, F Miletto Granozio, F Carillo, A Di Chiara, K Verbist and G Van Tendeloo, *Phys. Rev. B* **59** (1999) 11523; F Tafuri, F Carillo, F Lombardi, F Miletto Granozio, F Ricci, U Scotti di Uccio, A Barone, G Testa, E Sarnelli and J R Kirtley, *Phys. Rev. B* **62** (2000) 14431.
10. F Lombardi, F Tafuri, F Ricci, F Miletto Granozio, A Barone, G Testa, E Sarnelli, J R Kirtley and C C Tsuei, *Phys. Rev. Lett.* **89** (2002) 207001.
11. T Bauch, F Lombardi, F Tafuri, A Barone, G Rotoli, P Delsing and T Claeson, *Phys. Rev. Lett.* **94** (2005) 87003.
12. T Bauch, T Lindström, F Tafuri, G Rotoli, P Delsing, T Claeson and F Lombardi, *Science* **311** (2006) 57.
13. L B Ioffe, V B Geshkenbein, M V Feigel'man, A L Fauchere, and G Blatter *Nature* **398** (1999) 679; G Blatter, V B Geshkenbein, and L B Ioffe, *Phys. Rev. B* **63** (2001) 174511.
14. A Blais and A M Zagoskin, *Phys. Rev. A* **61** (2000) 42308; A Zagoskin, *cond-mat/0506039* 2005.
15. Y Makhlin, G Schon and A Shnirman, *Rev. Mod. Phys.* **73** (2001) 357.
16. A F Andreev, *Zh. Eksp. Teor. Fiz.* **46** (1964) 1823. (*Sov. Phys. JETP* **19** 1228); C -R. Hu, *Phys. Rev. Lett.* **72** (1994) 1526.
17. M Sigrist, *Progr. Theor. Physics* **99** (1998) 899; T

- Lofwander, V Shumeiko and G Wendin, *Supercond. Sci. Tech.* **14** (2001) R53; A A Golubov, M Yu Kupryanov and E Il'ichev, *Rev. Mod. Phys.* **76** (2004) 411; S Kashiwaya and Y Tanaka, *Rep. Prog. Phys.* **63** (2000) 1641.
18. E Il'ichev, V Zakosarenko, R P J Ijsselsteijn, H E Hoenig, V Schultze, H G Meyer, M Grajcar and R Hlubina, *Phys. Rev. B* **60** (1999) 3096; E Il'ichev, M Grajcar, R Hlubina, R P J Ijsselsteijn, H E Hoenig, H-G Meyer, A Golubov, M H S Amin, A M Zagoskin, A N Omelyanchouk and M Yu Kupriyanov, *Phys. Rev. Lett.* **86** (2001) 5369.
  19. T Lindstrom, S A Charlebois, A Ya Tzalenchuk, Z Ivanov, M H S Amin and A M Zagoskin, *Phys. Rev. Lett.* **90** (2003) 117002.
  20. Aya Tzalenchuk, T Lindstrom, S A Charlebois, E A Stepantsov, Z Ivanov and A M Zagoskin, *Phys. Rev. B* **68** (2003) 100501(R).
  21. M H S Amin, A Yu Smirnov, A M Zagoskin, T Lindström, S A Charlebois, T Claeson and A Ya Tzalenchuk, *Phys. Rev. B* **71** (2005) 064516.
  22. Ya V Fominov, A A Golubov and M Yu. Kypriyanov, *JETP Lett.* **77** (2003) 587.
  23. M H S Amin and A Yu Smirnov, *Phys. Rev. Lett.* **92** (2004) 17001.
  24. F Tafuri, J R Kirtley, F Lombardi and F Miletto Granozio, *Phys. Rev. B* **67** (2003) 174516.
  25. J Mannhart, H Hilgenkamp, B Mayer, Ch Gerber, J R Kirtley, K A Moler and M Sgrist, *Phys. Rev. Lett.* **77** (1996) 2782.
  26. H Hilgenkamp, J Mannhart and B Mayer, *Phys. Rev. B* **53** (1996) 14586; H J H Smilde, Ariando, D H A Blank, G J Gerritsma, H Hilgenkamp and H Rogalla, *Phys. Rev. Lett.* **88** (2002) 057004.
  27. M H Devoret, J M Martinis and J Clarke, *Phys. Rev. Lett.* **55** (1985) 1908; J M Martinis, M H Devoret and J Clarke, *Phys. Rev. B* **35** (1987) 4682.
  28. H A Kramers, *Physica (Utrecht)* **7** (1940) 284.
  29. A J Leggett, *J Phys. (Paris) Colloq.* **39** (1980) C6-1264; A O Caldeira and A J Leggett, *Ann. Phys. (N.Y)* **149** (1983) 374.
  30. W N Hardy, D A Bonn, D C Morgan, R Liang and K. Zhang, *Phys. Rev. Lett.* **70** (1993) 3999.
  31. G Lamura, E Di Gennaro, M Salluzzo, A Andreone, J Le Cochee, A Gauzzi, C Cantoni, M Paranthaman, D K Christen, H M Christen, G Giunchi and S Ceresara, *Phys. Rev. B* **65** (2002) 020506.
  32. A Andreone, A Cassinese, L Gianni, M Iavarone, F Palomba, and R Vaglio, *Phys. Rev. B* **64** (2001) 100505.
  33. A Fuchs, W Prusseit, P Berberich and H Kinder, *Phys. Rev. B* **53** (1996) R14745.
  34. A Carrington, R W Giannetta, J T Kim and J Giapintzakis, *Phys. Rev. B* **59** (1999) R14173.
  35. M R Trunin, *JETP Letters* **72** (2000) 583.
  36. A J Zaleski and J Klamut, *Phys. Rev. B* **59** (1999) 14023.
  37. E R Ulm, J-T Kim, T R Lemberger, S R Foltyn and X Wu, *Phys. Rev. B* **51** (1995) 9193.
  38. M Salluzzo, F Palomba, G Pica, A Andreone, I Maggio-Aprile, Ø Fischer, C Cantoni and D P Norton, *Phys. Rev. Lett.* **85** (2000) 1116.
  39. A Gauzzi, J Le Cochee, G Lamura, B J Jönsson, V A Gasparov, F R Ladan, B Plaçais, P A Probst, D Pavuna and J Bok, *Rev. Sci. Instrum.* **71** (2000) 2147.
  40. B Pümpin, et al., *Phys. Rev. B* **42**(1990) 8019.
  41. S-F Lee, D C Morgan, R J Ormeno, D M Broun, R A Doyle, J R Waldram and K Kadowaki, *Phys. Rev. Lett.* **77** (1996) 735.
  42. D A Bonn, R Liang, T M Riseman, D J Baar, D C Morgan, Kuan Zhang, P Dosanjh, T L Duty, A MacFarlane, G D Morris, J H Brewer, W N Hardy, C Kallin and A J Berlinsky, *Phys. Rev. B* **47** (1993) 11314.
  43. J Bardeen, N L Cooper and J R Schrieffer, *Phys. Rev.* **108** (1957) 1175.
  44. P W Anderson, *Phys. Rev. Lett.* **3** (1959) 325.
  45. P J Hirschfeld, W O Puttিকা, D J Scalapino, *Phys. Rev. B* **50** (1994) 10250.
  46. G Lamura, M Aurino, G Cifariello, E Di Gennaro, A Andreone, N Emery, C Hérold, J-F Marêché and P Lagrange, *Phys. Rev. Lett.* **96** (2006) 107008.
  47. J Bardeen, *Phys. Rev. Lett.* **1** (1958) 399.
  48. S K Yip and J A Sauls, *Phys. Rev. Lett.* **69** (1992) 2264.
  49. T Dahm and D J Scalapino, *Phys. Rev. B* **60** (1999) 13125.
  50. G Cifariello, M Aurino, E Di Gennaro, G Lamura, A Andreone, P Orgiani, X X Xi, and J-C Villégier, *Appl. Phys. Lett.* **88** (2006) 142510.
  51. D E Oates, S-H Park, and G Koren, *Phys. Rev. Lett.* **93** (2004) 197001.